Genus-Specific Carbon Fixation Activity Measurements Reveal Distinct Responses to Oxygen among Hydrothermal Vent *Campylobacteria*

Jesse McNichol,[a]* Stefan Dyksma,[b§] Marc Mußmann,[b◇] Jeffrey S. Seewald,[c] Sean P. Sylva,[c] Stefan M. Sievert[a]

aBiology Department, Woods Hole Oceanographic Institution, Woods Hole, Massachusetts, USA
bDepartment of Molecular Ecology, Max Planck Institute for Marine Microbiology, Bremen, Germany
cDepartment of Marine Chemistry and Geochemistry, Woods Hole Oceanographic Institution, Woods Hole, Massachusetts, USA

Jesse McNichol and Stefan Dyksma contributed equally to this work. Author order was arrived at by mutual agreement between Stefan Dyksma and Jesse McNichol.

ABSTRACT Molecular surveys of low temperature deep-sea hydrothermal vent fluids have shown that *Campylobacteria* (previously *Epsilonproteobacteria*) often dominate the microbial community and that three genera, *Arcobacter*, *Sulfurimonas*, and *Sulfurovum*, frequently coexist. In this study, we used replicated radiocarbon incubations of deep-sea hydrothermal fluids to investigate activity of each genus under three experimental conditions. To quantify genus-specific radiocarbon incorporation, we used newly designed oligonucleotide probes for *Arcobacter*, *Sulfurimonas*, and *Sulfurovum* to quantify their activity using catalyzed-reporter deposition fluorescence *in situ* hybridization (CARD-FISH) combined with fluorescence-activated cell sorting. All three genera actively fixed CO_2 in short-term ($\sim$ 20 h) incubations, but responded differently to the additions of nitrate and oxygen. Oxygen additions had the largest effect on community composition, and caused a pronounced shift in community composition at the amplicon sequence variant (ASV) level after only 20 h of incubation. The effect of oxygen on carbon fixation rates appeared to depend on the initial starting community. The presented results support the hypothesis that these chemoautotrophic genera possess functionally redundant core metabolic capabilities, but also reveal finer-scale differences in growth likely reflecting adaptation of physiologically-distinct phylotypes to varying oxygen concentrations *in situ*. Overall, our study provides new insights into how oxygen controls community composition and total chemoautotrophic activity, and underscores how quickly deep-sea vent microbial communities respond to disturbances.

IMPORTANCE Sulfidic environments worldwide are often dominated by sulfur-oxidizing, carbon-fixing *Campylobacteria*. Environmental factors associated with this group's dominance are now understood, but far less is known about the ecology and physiology of members of subgroups of chemoautotrophic *Campylobacteria*. In this study, we used a novel method to differentiate the genus-specific chemoautotrophic activity of three subtypes of *Campylobacteria*. In combination with evidence from microscopic counts, chemical consumption/production during incubations, and DNA-based measurements, our data show that oxygen concentration affects both community composition and chemoautotrophic function *in situ*. These results help us better understand factors controlling microbial diversity at deep-sea hydrothermal vents, and provide first-order insights into the ecophysiological differences between these distinct microbial taxa.

KEYWORDS arcobacter, CARD-FISH, Campylobacteria, chemoautotrophy, deep-sea hydrothermal vents, FACS, niche differentiation, sulfur oxidation, Sulfurimonas, Sulfurovum

In deep-sea hydrothermal vent ecosystems and other sulfidic, low-oxygen environments, one of the most abundant and biogeochemically important bacterial groups is the *Campylobacteria* (previously known as *Epsilonproteobacteria*) (1), whose dominance at vents was first reported 25 years ago (2–4). Environmental surveys in sulfidic cave systems and at hydrothermal vents have consistently shown that *Campylobacteria* occupy a high-sulfide, low-oxygen niche compared with chemoautotrophic *Gammaproteobacteria* (5, 6), but less is known about factors driving niche differentiation within the *Campylobacteria*. At a broad level, genomic analyses have revealed that the *Campylobacteria* can be divided into two major orders that have clear differences in their metabolic potential and core bio-energetics. The first order, the *Nautiliales*, was the first to be isolated in pure culture from hydrothermal vents and was originally described as moderately thermophilic hydrogen-dependent obligate anaerobes or microaerophiles that tolerate or use a small amount of oxygen (7, 8), though aerobic representatives have been more recently identified (9). The second order, the *Campylobacterales*, were initially isolated from both vent systems (10, 11) and coastal sediments (12–14). In contrast to the *Nautiliales*, most cultured representatives of the *Campylobacterales* thrive at lower temperatures and can typically tolerate a much greater range of oxygen concentrations ([15] and references therein).

In contrast to these broad, interorder or interclass differences in physiology, much less is known about differences in metabolism between members of the *Campylobacterales* and factors governing their co-existence in the natural environment. At our study site (Crab Spa), both the chemical composition of hydrothermal fluids (16, 17) and the micro-bial population structure has remained relatively stable over a period of 1 year (18). Similar to other diffuse-flow hydrothermal vents, the microbial community of the sub-seafloor-derived fluid of Crab Spa is primarily dominated by the three genera of *Campylobacterales*: *Arcobacter*, *Sulfurimonas*, and *Sulfurovum* (6, 18–25). (Although currently classified as gen-era, we point out to readers that these names. in particular *Sulfurovum*, represent broader phylogenetic groupings as noted by others [6] and are likely to be changed in the future.)

Information on the physiology of these organisms comes primarily from pure cul-ture studies which have shown that isolates of *Sulfurimonas* and *Sulfurovum* typically use H_2 and reduced sulfur compounds as electron donors and nitrate, sulfur, and oxy-gen as electron acceptors ([15] and references therein). Despite this relatively limited repertoire of substrates, isolates differ with respect to the presence/absence of path-ways. For example, some isolates are strict microaerobes, whereas others can use ni-trate as an alternative electron acceptor. In addition, oxygen tolerance varies markedly (even within the same genus), with cultured representatives spanning a spectrum from obligate anaerobe (26) to obligate aerobes that can tolerate high levels of oxygen in the presence of high exogenous CO_2 concentrations (27). Environmental surveys and short-term incubations have also underscored the importance of oxygen in structuring natural communities and affecting carbon fixation efficiency (6, 18).

Much less is known about *Arcobacter* because no chemoautotrophic isolate exists. Based on enrichment cultures, it has been inferred to be a chemoautotroph possibly thriving under highly turbulent and sulfidic conditions (28, 29). Modern omics surveys and the genome reconstructions have similarly shown that the same general pathways are present for diverse *Campylobacteria* (6, 30, 31) and that they are transcriptionally active (31, 32). However, few studies have directly measured primary production under conditions reflective of natural environments (18), much less at a resolution possible to distinguish differences between genera of *Campylobacteria*. Thus, the factors driving the activity and chemoautotrophic carbon fixation in the natural environment remain largely unknown.

To better quantify the activity of these three genera in diffuse-flow hydrothermal fluids under varying conditions, we applied a recently developed method for the quantification of genus-specific radiocarbon incorporation (33) in combination with newly designed oligonu-cleotide probes to quantify genus-specific carbon fixation activity under three distinct and replicated experimental conditions. Combined with concurrent chemical measurements
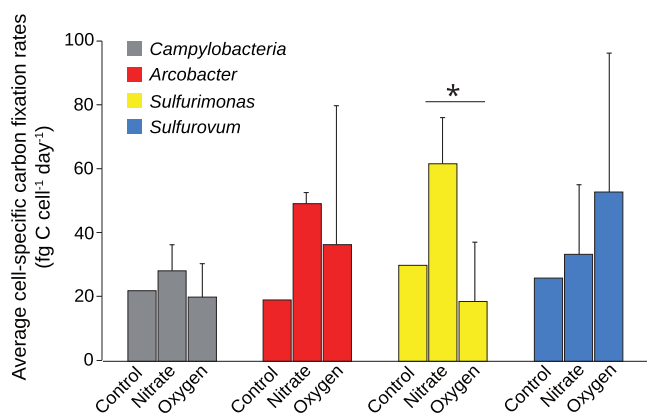
FIG 1 Cell-specific carbon fixation rates averaged over the replicates (control $n = 2$; nitrate $n = 3$, oxygen $n = 3$; see also Fig. S1 in the supplemental material). Error bars represent the standard deviation. Average carbon fixation rates that significantly differ ($P < 0.05$) between the treatments were labeled with an asterisk.

and molecular data, this work provides new insights into the activity and ecophysiology of *Campylobacterales* at deep-sea hydrothermal vents.

RESULTS AND DISCUSSION

The results presented here clearly show that *Campylobacteria*, and in particular the three genera *Arcobacter*, *Sulfurimonas*, and *Sulfurovum*, dominated chemoautotrophic carbon fixation at Crab Spa (Fig. 1 and Fig. S1). Similar to previously published data (17, 34), active microbial metabolism in the paired incubations was apparent based on the rapid consumption of sulfide, nitrate, and oxygen at similar rates. Control incubations (no additions) were limited by electron acceptors as demonstrated by the cessation of sulfide consumption after oxygen and nitrate (in that order) were successively drawn down (Fig. 2a, left panel). In contrast, in oxygen/nitrate addition experiments where electron acceptors were not limiting, sulfide was continuously consumed (Fig. 2a, middle and right panel). Determining reaction stoichiometry by making comparisons of nitrate/oxygen consumption as described in (17) is not straightforward for these incubations because oxygen was supplied from the headspace and measured in the fluids. Thus, oxygen drawdown as shown in Fig. 2a likely underestimates the total amount of oxygen consumed. The fraction of nitrate likely processed through the dissimilatory nitrate reduction to ammonium (DNRA) pathway varied considerably between the three replicates to which nitrate was added (sample no. 4769-4 = 48%, sample no. 4770-8 = 12%, sample no. 4773-5 = 31%; values are corrected to account for ~15 fg ammonium uptake per new cell), with the remainder presumably being denitrified to N_2.

At the end of the incubations, CARD-FISH and amplicon sequences (ASVs summed within each genus) showed that the three target genera *Sulfurimonas*, *Sulfurovum*, and *Arcobacter* were all present and each comprised > 20% of total cell counts/ASV sequences in at least one incubation (Fig. 2b, 3, and Fig. S2). This was not the case in incubations conducted at *in situ* pressure earlier in the same year at the same study site (18). In those incubations, amplicon sequences and CARD-FISH cell numbers showed that *Sulfurimonas* (and to a lesser extent *Thioreductor*, a member of the *Nautiliales*) dominated activity and biomass, whereas *Arcobacter* and *Sulfurovum* were always present at < 20% relative abundance of ASV sequences at the end of incubations across 18 biological replicates (18). Those *in situ* pressure incubations did not measure the starting community composition as we reported here, but given that *Arcobacter* and *Sulfurovum* are always present in initial samples (Fig. 2b), it appears likely that the robust growth of these taxa in our incubations at atmospheric pressure is an effect specific to our experimental setup, possibly indicating that *Sulfurovum* and *Arcobacter* might be less affected by pressure changes or adapted better to the additional
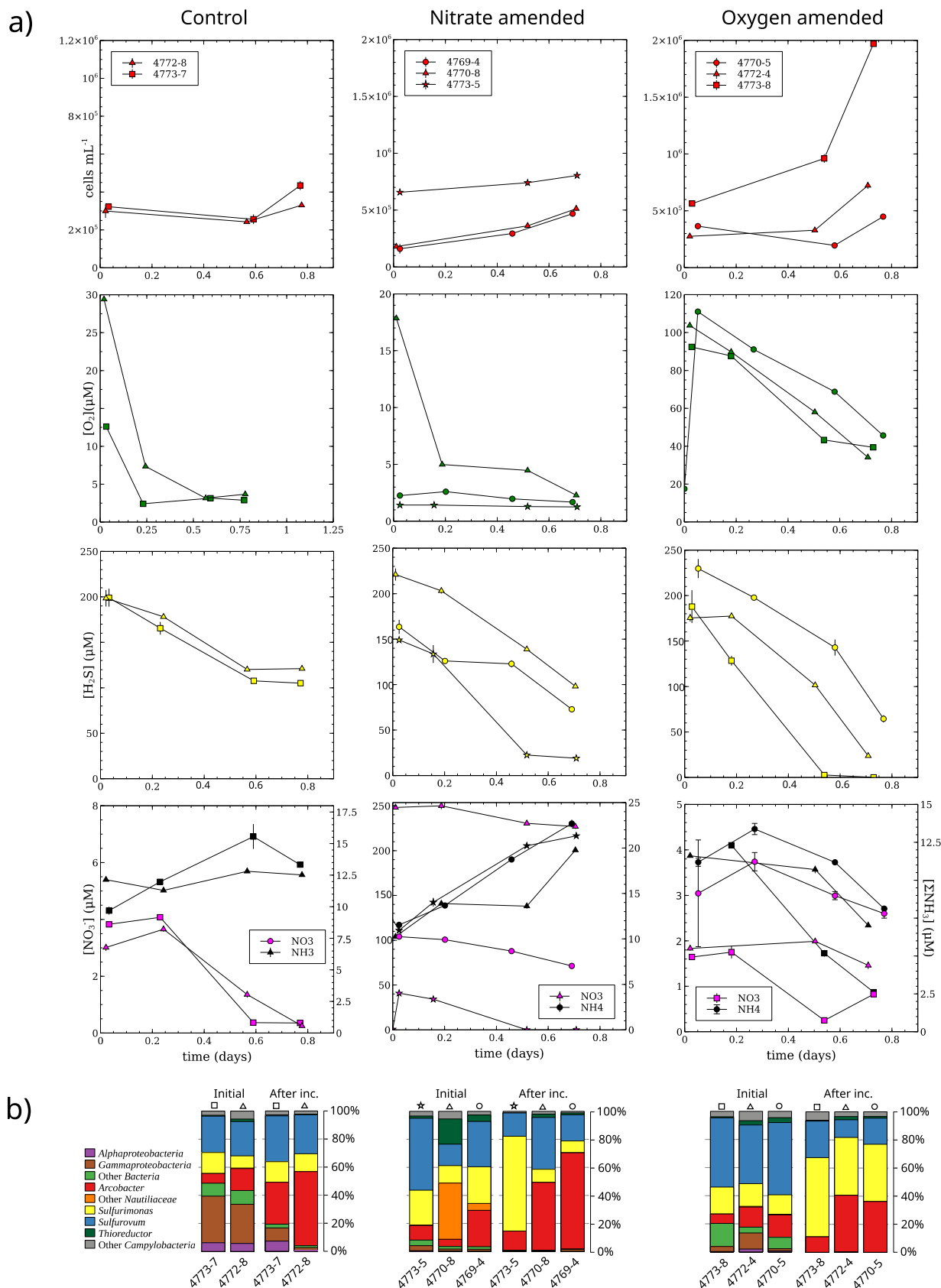
FIG 2 Chemical and biological parameters in simultaneous nonradioactive incubations (a). Cell numbers and the concentration of potential electron donors/acceptors were determined over the incubation period. The microbial community composition in the initial fluids and after incubation was determined by 16S rRNA gene amplicon sequencing (b).
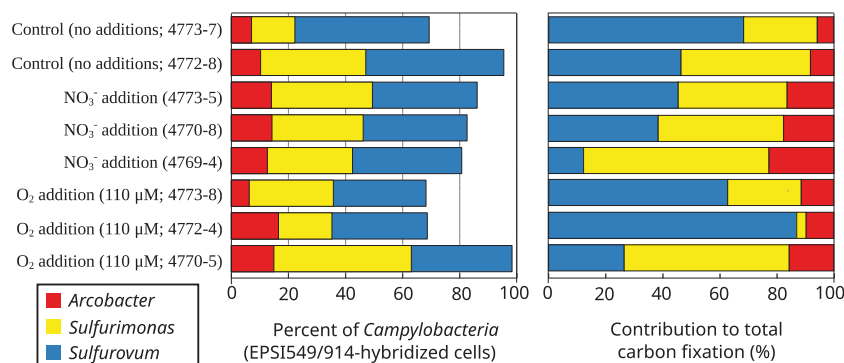
FIG 3 Percentages of total cells identified in radiocarbon incubations using CARD-FISH and their predicted relative contributions to carbon fixation within *Campylobacteria* based on cell-specific rate measurements.

fluid handling. These differing incubation conditions might also explain the lack of growth of *Thioreductor* in this study, but we note that the abundance of related organisms is more variable (see for e.g., *Nautiliales* in Fig. 2b 4770-8, initial time point), meaning that the effect of initial community composition might be more important for growth of these putatively thermophilic taxa in incubations.

Carbon fixation rates. Based on all sorted *Campylobacteria* (EPSI 549/914-hybridized), the average cell-specific carbon fixation rates across all replicates and treatments ranged from 13 to 36.3 fg C cell^{-1} day^{-1} (average = 23.6 $\pm$ 8.5 [standard deviation here and following]; $n = 8$; Fig. 1), which were significantly lower ($P < 0.01$) compared with rates previously measured by NanoSIMS in incubations conducted at *in situ* pressure with isobaric gas-tight samplers which underwent a similar CARD-FISH hybridization procedure (25.4 – 134.2, average = 78.4 $\pm$ 25.3 fg C cell^{-1} day^{-1}; $n = 18$; [18]). This could possibly indicate a pressure effect, although additional fluid handling could also play a role.

Evidence of high chemoautotrophic activity and the ability to respond rapidly to changing conditions for *Arcobacter*. Chemoautotrophic *Arcobacter* have been characterized as microaerophilic sulfur-oxidizing bacteria that can tolerate high sulfide and produce copious amounts of sulfur in filamentous form (28, 35, 36). Similar organisms have been suggested to be important players in highly turbulent environments with high sulfide concentrations, such as those found after a volcanic eruption (20, 29). In our incubations, we observed evidence of growth and carbon fixation for *Arcobacter*-affiliated organisms. The relative abundance of 16S rRNA gene amplicons affiliating with *Arcobacter* increased in most incubations independent of the treatment (Fig. 2b), indicating cell growth. Supporting this, only a few *Arcobacter* ASVs were dominant at the end of incubations compared with the beginning and were completely distinct between oxygen-amended and the other incubations (Fig. S3a). This suggests quick growth of a relatively small number of phylotypes within this genus that are adapted to different oxygen concentrations *in situ*.

One of the highest cell-specific carbon fixation rates was determined for *Arcobacter* in the incubation 4773-8 (86.2 fg C cell^{-1} d^{-1}; Fig. S1). In this incubation, one particular ASV became abundant that was not observed in other incubations (Fig. S3a). The *Arcobacter* average community cell-specific rate is considerably higher than the value of 14.4 fg C cell^{-1} d^{-1} previously reported for *Candidatus Arcobacter sulfidicus* (35), which indicates these organisms were growing well under our incubation conditions. Although the average cell-specific carbon fixation rates for *Arcobacter* were comparable with those of *Sulfurimonas* and *Sulfurovum* (*Arcobacter*, 36.8 fg C cell^{-1} d^{-1}; *Sulfurimonas*, 37.5 fg C cell^{-1} d^{-1}; *Sulfurovum*, 38.8 fg C cell^{-1} d^{-1}), they only contributed 5.7% to 23% to total carbon fixed due to their lower overall cell numbers (Fig. 3). Despite lower cell abundances, *Arcobacter* represented a larger fraction of total amplicon sequences and were more likely to be composed of only one or a few ASVs compared with *Sulfurimonas* and *Sulfurovum*
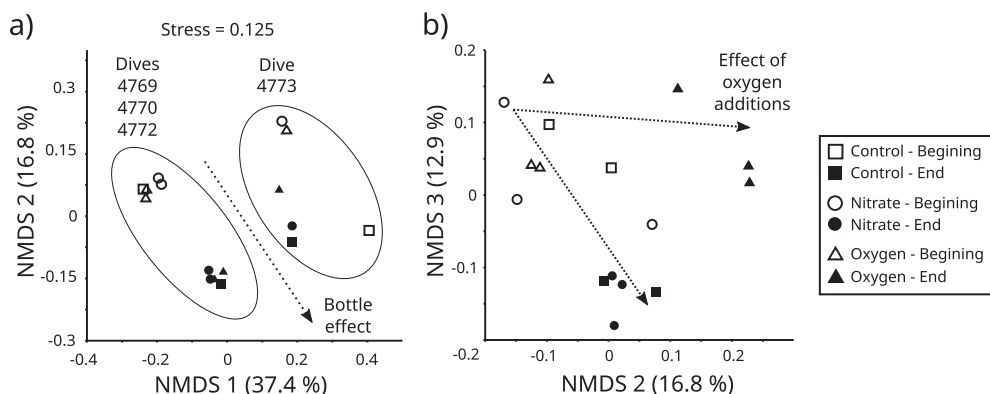
FIG 4 Nonmetric multidimensional scaling (NMDS) plots showing changes in campylobacterial community composition across incubations and sampling time. Panel (a) shows the major community difference between Alvin dive 4773 and other dives which is likely attributed to the deployment of an *in situ* sampling device (discussed in text), as well as a clear "bottle effect" for all samples. Panel (b) shows a reproducible effect of oxygen on community composition regardless of dive.

(Fig. S3a to c). Considering the ratio of ASV abundance to CARD-FISH cell numbers, we found that *Arcobacter* had the highest and most variable ratio (2.1 $\pm$ 1.3), whereas the ratio for both *Sulfurimonas* and *Sulfurovum* was close to 1:1 on average (1.2 $\pm$ 0.5 and 1.0 $\pm$ 0.1, respectively). This observation indicates *Arcobacter* has a higher average 16S rRNA gene copy number per genome compared with *Sulfurimonas* and *Sulfurovum*, a proxy for bacterial adaption to resource availability (37). Together, these data support the previous speculation that *Arcobacter* can rapidly respond to changing conditions (28, 29), though it seems that at least some members of all three genera have the same potential to respond rapidly (Fig. S3b to c).

Sulfurimonas and Sulfurovum account for the majority of carbon fixation. *Sulfurimonas* and *Sulfurovum* accounted for the majority of carbon fixation due to their high cell abundances in the incubations (Fig. 3), in line with studies showing they are the dominant microorganisms in diffuse-flow hydrothermal fluids (6, 18–25, 38). Compared with *Arcobacter*, the contribution of *Sulfurimonas and Sulfurovum* to total carbon fixation was significantly higher ($P <$ 0.01), accounting for 39.5% $\pm$ 21.7% and 47.8% $\pm$ 25.1%, respectively (Fig. 3). During the incubations, both *Sulfurimonas* and *Sulfurovum* mostly maintained a relatively high diversity, but an effect of incubation could still be observed with different ASVs coming to dominate at the end of incubations (in particular for incubation 4773-5; Fig. S3b, c). Average cell-specific carbon fixation rates for *Sulfurimonas* were consistently higher with nitrate additions (61.5 $\pm$ 14.4 fg C cell^{-1} d^{-1}) compared with oxygen additions (18.6 $\pm$ 18.5 fg C cell^{-1} d^{-1}) ($P <$ 0.05; Fig. 1), whereas carbon fixation for *Sulfurovum* appeared to be stimulated by O$_2$ (Fig. 1). We observed the highest cell-specific carbon fixation rates for *Sulfurovum* in oxygen amended incubations (92.2 fg C cell^{-1} d^{-1}; Fig. S1), and note that these rates were substantially higher compared to *Sulfurimonas*. This presumably aerobic metabolism is consistent with a report showing positive correlations between oxygen and the abundance of *Sulfurovum*-related sequences in natural systems (6).

Chemoautotrophic rates and community composition were most influenced by oxygen. ASV analysis revealed that the final community compositions in oxygen amendments diverged markedly from control and nitrate additions in a consistent manner for samples taken across all dives (Fig. 4 and Fig. S3). This supports the notion that oxygen concentration is a major physicochemical factor determining community structure *in situ*, in line with observations from environmental surveys and incubation studies (6, 18). A clear "bottle effect" could also be observed, with the composition diverging markedly from the initial state even for no-amendment controls (Fig. 4).

The effect of oxygen on community carbon fixation appeared to be linked to the initial community composition in the sampled fluids. Although the microbial community sampled at Crab Spa was consistent across the first three Alvin dives, we observed a large difference in campylobacterial community composition (Fig. 4 and Fig. S3) and

lower alpha diversity (Fig. S4) for the sample taken during dive 4773. There was essentially no overlap in ASVs among the initial communities sampled during the first three dives and the last sample (Fig. S3), indicating that a community shift occurred at Crab Spa at a fine-scale taxonomic level. In addition, we observed higher cell-specific carbon fixation rates for all three campylobacterial genera in the oxic incubation with fluids sampled during dive 4773, compared with fluids sampled during dive 4770 and 4772 (Fig. S1). While we cannot exclude sampling differences or other stochastic factors to have played a role, we think it is likely that this could be related to a disturbance caused by the deployment of an instrument between dives 4772 and 4773. Assuming that taxa initially present in fluids obtained on dive 4773 were more tolerant to oxygen, this suggests that both oxygen tolerance and carbon fixation efficiency for *Campylobacteria* may not be easily generalized because both appear to depend on the composition of the *in situ* microbial community. While this conclusion requires further studies to confirm, it is consistent with experimental evidence showing that oxygen affects campylobacterial growth and carbon fixation efficiency in a taxon-specific manner (6, 15, 18).

Conclusions. In this study, we obtained genus-specific chemoautotrophic carbon fixation rates for *Arcobacter*, *Sulfurimonas*, and *Sulfurovum*, the three dominant chemoautotrophic genera commonly observed in diffuse-flow hydrothermal vent fluids and other sulfidic environments. We also observed that all three genera were simultaneously active in our incubations, that oxygen had the largest effect on microbial community composition on short time-scales, and that the effect of oxygen on carbon fixation rates/efficiency is likely dependent on the specific community members present. This demonstrates that despite our study site's chemical stability over time, it retains community members that can respond rapidly to changing conditions, most likely due to adaptations to tolerate differing *in situ* oxygen levels. This observation is consistent with data showing that *Sulfurovum* and *Sulfurimonas* are much more diverse at a genomic level compared with gammaproteobacterial sulfur oxidizers of the SUP05 clade found in more oxic seawater surrounding hydrothermal vents (6). This greater campylobacterial diversity has been suggested to be due the wide range of microniches made available during mixing of hydrothermal fluids with seawater (6).

In the future, investigation of precise environmental conditions, environmental genomic diversity, and concerted isolation campaigns could help reveal further reasons for the co-existence of these three taxa and maintenance of high microdiversity among chemoautotrophic *Campylobacteria*. It is likely that previously implied differences in enzyme substrate specificity (6, 39) and the ability to move to physiologically optimal microenvironments (28) are extremely important factors. In addition, more subtle and less well-explored features may include size (24) and arrangement of cells (26) which would likely have important implications for attachment to solid substrates, the ability to compete for limiting nutrients, or avoiding grazing/viral infection.

MATERIALS AND METHODS

Hydrothermal fluid sampling and paired/radiocarbon incubations. Fluid samples were collected from the low-temperature hydrothermal vent Crab Spa (16–18) using isobaric gas tight (IGT) samplers (40) deployed by the HOV *Alvin*. Crab Spa is part of the East Pacific Rise 9°N vent field (9°50.3981 N, 104° 17.4942 W; 2,506 m), and its fluids vent at a stable temperature of 24°C. The use of radiocarbon to measure carbon fixation is hereafter referred to as "radiocarbon incubations." Synchronized nonradioactive incubations (with the same source fluids and headspace:liquid ratio) were also carried out to measure additional chemical and biological parameters (cell numbers, CARD-FISH, 16S rRNA gene amplicon sequencing) and the concentration of potential electron donors/acceptors and metabolic by-products over the incubation period. These are referred to as "paired incubations" below. Sample incubations were started on average ∼7 h after sampling on the seafloor (Table 1). To simulate three different redox conditions, we either made no additions or provided nitrate/oxygen as amendments. We chose to add electron acceptors rather than donors because the fluid chemistry of Crab Spa is characterized by high sulfide concentrations ($\sim$180μM ΣH_2S; [16, 17]) relative to oxygen and nitrate (O_2 $\sim$3 μM; NO_3^- $\sim$6 μM), leading to electron acceptor limitation of sulfide-oxidizing chemoautotrophs (17).

For radiocarbon incubations, 8 mL of hydrothermal fluid was transferred from the IGTs into 12 mL N_2-flushed exetainer screw cap vials (Labco Limited) and spiked with ^{14}C sodium bicarbonate (specific activity 56 mCi mmol^{-1}, Hartmann Analytic, Germany) resulting in a final radioactive dissolved inorganic

TABLE 1 Summary of conditions during atmospheric pressure incubations using IGT fluid samplers

Amendment	Concn (μM)	Temp (°C)	# Replicates	Time from seafloor[a] (h)	Experimental IDs (Alvin dive #s, IGT ID)
Control	NA	24	2	7.3, 5.1	4772-8, 4773-7
Nitrate	100–200	24	3	9.3, 6.2, 8.4	4769-4, 4770-8, 4773-5
Oxygen	110	24	3	4.6, 9.3, 7.0	4770-5, 4772-4, 4773-8

[a]Time from sampling at seafloor to beginning of incubation.

carbon (DIC) fraction of 0.17%. Fluid DIC concentrations for this calculation were from previous measurements at the same study site (17). All vials were incubated for 16 h at *in situ* temperature (24°C) in the dark after which cells were fixed with formaldehyde (2%, final concentration) for 1 h at room temperature. For paired incubations, approximately 80 mL of hydrothermal fluid was transferred with a sterile needle directly from the IGT into a N_2-purged 123 mL GL45 Pyrex flask sealed with a ~2-cm thick butyl stopper (Part #444704, Glasgerätebau Ochs, Germany), and excess N_2 overpressure released with another sterile needle at the end of filling. Flasks were rinsed with MilliQ water between incubations, and sterilized by contact with 70% ethanol and subsequent drying in a 50°C oven. In both radiocarbon and paired incubations, nitrate was added as a small aliquot of a N_2-purged 0.175 M $NaNO_3$ solution, and O_2 was added as gas directly to the headspace to reach an initial concentration of dissolved O_2 of approximately 100 μM. Concentrations of dissolved O_2 were calculated as described previously (41).

Cell counts and chemical measurements (H_2S, NO_3^-, O_2; only for paired incubations) were conducted as previously described (17) except oxygen was measured with the Fibox 3 instrument using an optode spot affixed to the inside of the bottle using silicone (Pts3, PreSens, Regensburg, Germany). Subsamples were taken with sterile needles/syringes that were purged with 0.2 μm-filtered N_2 gas three times prior to sampling. The same volume of sterile N_2 gas as the fluid sample was injected to prevent underpressure forming in the incubation vessels.

CARD-FISH and sample preparation for flow cytometry. Samples from radiocarbon incubations were filtered onto 25-mm diameter polycarbonate membrane filters with a 0.2-μm pore size (GTTP, Millipore, Eschborn, Germany). Permeabilization and CARD-FISH was performed as described previously (42) with the following modifications. Samples for flow cytometry were not embedded in agarose. Endogenous peroxidases were inactivated in 3% H_2O_2 for 10 min at room temperature. The hybridization temperature was 46°C and washing was performed at 48°C according to the protocol of Ishii et al. (43). An overview of oligonucleotide probes used in this study is shown in Table S1. Tyramides labeled with Alexa Fluor 488 fluorescent dye (Molecular Probes, USA) were used for CARD signal amplification. Cells were removed from filter membranes using a cell scraper or were vortexed in 5 mL of 150 mM NaCl containing 0.05% Tween 80 according to Sekar et al. (44). Prior to flow cytometry, large, suspended particles were removed by filtration through 8-μm pore size filter (Sartorius, Göttingen, Germany) to avoid clogging of the flow cytometer.

Fluorescence activated cell sorting and scintillation counting. Flow sorting of CARD-FISH-identified cells and scintillation counting of sorted cell fractions were performed as described previously (33). In brief, cells were sorted using a FACSCalibur flow cytometer (Becton Dickinson, Oxford, UK) in batches of at least 10,000 cells. Hybridized cells were identified on scatter dot plots of green fluorescence versus 90° light scatter and background was determined by flow cytometric analysis of hybridizations with a nonsense probe (NON338) prior to flow sorting. Sorted cell batches that were collected on polycarbonate filters were transferred into 5 mL scintillation vials and mixed with 5 mL UltimaGold XR (Perkin Elmer, Boston, MA, USA) scintillation cocktail. Radioactivity of sorted cell batches was measured in a liquid scintillation counter (Tri-Carb 2900, Perkin Elmer, USA). Average cell-specific carbon fixation rates were calculated according to the equation $R = (A*M)/(a*n*t*L)$. *A* represents the radioactivity of the sorted cell batch in Becquerel (Bq), *M* represents the molar mass of carbon (g/mol), *a* represents the specific activity of the tracer (Bq/mol), *n* represents the number of sorted cells, *t* represents the incubation time, and *L* equals to the ratio of total DIC to ^{14}C-DIC. This population cell-specific average represents a slightly different calculation compared with studies that measure single-cell incorporation and average across all individually measured cell uptake rates. Another key difference of this technique versus single-cell assays is that tens of thousands of cells can be sorted and quantified precisely versus dozens to hundreds for techniques such as NanoSIMS. Two sample t-tests were performed to determine if there were any differences in rates between treatments.

CARD-FISH probe design and testing. To demarcate the regions of the SILVA reference tree (version: "SILVA_119_SSURef_Nr99") to target for probe design, steps from the ARB tutorial by Amy Apprill (http://www.arb-home.de/documentation.html) were used as a template. Briefly, partial 16S rRNA genes derived from PCR amplicons sequenced with 454 technology (from the Atlantis cruise AT26-10 [18]) were first aligned with the SINA web aligner (45). Clusters without partial 16S rRNA sequences derived from AT26-10 were removed (e.g., those containing *Sulfurimonas denitrificans* and *Sulfurimonas gotlandica* that occur in nonvent environments) and the remaining sequences were used for probe design.

Candidate probe sequences were selected based on coverage of the relevant genera (*Arcobacter*, *Sulfurimonas*, and *Sulfurovum*), and helper/competitor probes were also designed to assist with specific binding (Table S1). Probes were tested *in silico* against full-length clone sequences derived from the same vent field (22) and also (where applicable) partial 16S SSU rRNA amplicon sequences derived from

single-amplified genomes sorted by the Bigelow Single-Cell Genomics Center (unpublished data). We note that although probes already existed for *Arcobacter* (ARC94 and ARC1430 [35, 46]), they only cover about 80% of *Arcobacter* sequences found in SILVA SSU database r138 (47). In addition, ARC94 has unacceptable outgroup matches to *Nitratiruptoraceae* (67% coverage) and *Thioreductoraceae* (100% coverage), both members of the *Nautiliales* which have markedly different physiologies compared with *Arcobacter* and have been shown to be present alongside *Sulfurimonas* at least under some conditions (18). In contrast, our newly designed *Arcobac*ter probe (ARC673) increases group coverage to ~94% and has no significant outgroup matches.

To determine the optimum formamide concentration for hybridization, probes (with helpers and competitor oligonucleotides) were tested across a formamide melting curve with positive controls and 1-mismatches as described in Table S1. To ensure that probes only hybridized with *Campylobacteria* and did not cross-hybridize between genera or to non-campylobacterial cells, a series of double-hybridizations were carried out with each of the new probes in combination with either EPSI549/914 or each other. These were carried out on background (unincubated) samples from Crab Spa. Images of these double-hybridizations and CARD-FISH counts from experiments are available online at https://osf.io/yts4p/.

16S rRNA sequence analysis. DNA extraction and sequencing was as described in McNichol et al. (18) for low-volume extractions of biomass captured on a 0.2-μm pore size Sterivex filter and subsequent 454 amplicon sequencing of the 16S rRNA gene with the 27Fmod/519Rmodbio primers. Raw fastq files were manually de-multiplexed from SFFs file using qiime1 (48), and imported into qiime2 (2018.8 build; [49]). Sequences were denoised using the q2-DADA2 plugin (50), and classified using the naive Bayesian classifier (51) in qiime2 using SILVA 132 as a reference database (47) subsetted to the primer region. All scripts and accessory files needed to reproduce this analysis are available at https://osf.io/9e6ra/. Alpha diversity analysis and NMDS plots were made with PAST (52) using an ASV table subsetted to include only *Campylobacteria*.

Data availability. Raw fastq files split by sample were deposited at the NCBI SRA under BioProject number PRJNA505918.

SUPPLEMENTAL MATERIAL

Supplemental material is available online only.

SUPPLEMENTAL FILE 1, PDF file, 0.3 MB.

REFERENCES

1. Waite DW, Vanwonterghem I, Rinke C, Parks DH, Zhang Y, Takai K, Sievert SM, Simon J, Campbell BJ, Hanson TE, Woyke T, Klotz MG, Hugenholtz P. 2017. Comparative genomic analysis of the class Epsilonproteobacteria and proposed reclassification to Epsilonbacteraeota (phyl. nov.). Front Microbiol 8:682. https://doi.org/10.3389/fmicb.2017.00682.

2. Haddad A, Camacho F, Durand P, Cary SC. 1995. Phylogenetic characterization of the epibiotic bacteria associated with the hydrothermal vent polychaete Alvinella pompejana. Appl Environ Microbiol 61:1679–1687. https://doi.org/10.1128/aem.61.5.1679-1687.1995.

3. Moyer CL, Dobbs FC, Karl DM. 1995. Phylogenetic diversity of the bacterial community from a microbial mat at an active, hydrothermal vent system, Loihi Seamount, Hawaii. Appl Environ Microbiol 61:1555–1562. https://doi.org/10.1128/aem.61.4.1555-1562.1995.

4. Polz MF, Cavanaugh CM. 1995. Dominance of one bacterial phylotype at a Mid-Atlantic Ridge hydrothermal vent site. Proc Natl Acad Sci U S A 92: 7232–7236. https://doi.org/10.1073/pnas.92.16.7232.

5. Macalady JL, Dattagupta S, Schaperdoth I, Jones DS, Druschel GK, Eastman D. 2008. Niche differentiation among sulfur-oxidizing bacterial populations in cave waters. ISME J 2:590–601. https://doi.org/10.1038/ismej.2008.25.

6. Meier DV, Pjevac P, Bach W, Hourdez S, Girguis PR, Vidoudez C, Amann R, Meyerdierks A. 2017. Niche partitioning of diverse sulfur-oxidizing bacteria at hydrothermal vents. ISME J 11:1545–1558. https://doi.org/10.1038/ismej.2017.37.

7. Miroshnichenko ML, Kostrikina NA, L'Haridon S, Jeanthon C, Hippe H, Stackebrandt E, Bonch-Osmolovskaya EA. 2002. Nautilia lithotrophica gen. nov., sp. nov., a thermophilic sulfur-reducing epsilon-proteobacterium isolated from a deep-sea hydrothermal vent. Int J Syst Evol Microbiol 52:1299–1304.

8. Miroshnichenko ML, L'Haridon S, Schumann P, Spring S, Bonch-Osmolovskaya EA, Jeanthon C, Stackebrandt E. 2004. Caminibacter profundus sp. nov., a novel thermophile of Nautiliales ord. nov. within the class 'Epsilonproteobacteria', isolated from a deep-sea hydrothermal vent. Int J Syst Evol Microbiol 54: 41–45. https://doi.org/10.1099/ijs.0.02753-0.

9. Winkel M, Pjevac P, Kleiner M, Littmann S, Meyerdierks A, Amann R, Mußmann M. 2014. Identification and activity of acetate-assimilating bacteria in diffuse fluids venting from two deep-sea hydrothermal systems. FEMS Microbiol Ecol 90:731–746. https://doi.org/10.1111/1574-6941.12429.

10. Campbell BJ, Jeanthon C, Kostka JE, Luther GW, Cary SC. 2001. Growth and phylogenetic properties of novel bacteria belonging to the epsilon subdivision of the proteobacteria enriched from Alvinella pompejana and deep-sea hydrothermal vents. Appl Environ Microbiol 67:4566–4572. https://doi.org/10.1128/AEM.67.10.4566-4572.2001.

11. Takai K, Inagaki F, Nakagawa S, Hirayama H, Nunoura T, Sako Y, Nealson KH, Horikoshi K. 2003. Isolation and phylogenetic diversity of members of previously uncultivated epsilon-Proteobacteria in deep-sea hydrothermal fields. FEMS Microbiol Lett 218:167–174. https://doi.org/10.1111/j.1574-6968.2003.tb11514.x.

12. Timmer-Ten Hoor A-T. 1975. A new type of thiosulphate oxidizing, nitrate reducing microorganism: Thiomicrospira denitrificans sp. Nov. Netherlands J Sea Res 9:344–350. https://doi.org/10.1016/0077-7579(75)90008-3.

13. Muyzer G, Teske A, Wirsen CO, Jannasch HW. 1995. Phylogenetic relationships of Thiomicrospira species and their identification in deep-sea hydrothermal vent samples by denaturing gradient gel electrophoresis of 16S rDNA fragments. Arch Microbiol 164:165–172. https://doi.org/10.1007/BF02529967.

14. Takai K, Suzuki M, Nakagawa S, Miyazaki M, Suzuki Y, Inagaki F, Horikoshi K. 2006. Sulfurimonas paralvinellae sp. nov., a novel mesophilic, hydrogen- and sulfur-oxidizing chemolithoautotroph within the epsilonproteobacteria isolated from a deep-sea hydrothermal vent polychaete nest, reclassification of thiomicrospira denitrificans as sulfurimonas denitrificans comb. nov. and emended description of the genus sulfurimonas. Int J Syst Evol Microbiol 56:1725–1733. https://doi.org/10.1099/ijs.0.64255-0.

15. Sievert SM, Vetriani C. 2012. Chemoautotrophy at deep-sea vents: past, present, and future. Oceanog 25:218–233. https://doi.org/10.5670/oceanog.2012.21.

16. Reeves EP, McDermott JM, Seewald JS. 2014. The origin of methanethiol in midocean ridge hydrothermal fluids. Proc Natl Acad Sci U S A 111: 5474–5479. https://doi.org/10.1073/pnas.1400643111.

17. McNichol J, Sylva SP, Thomas F, Taylor CD, Sievert SM, Seewald JS. 2016. Assessing microbial processes in deep-sea hydrothermal systems by incubation at in situ temperature and pressure. Deep Sea Res Pt I 115: 221–232. https://doi.org/10.1016/j.dsr.2016.06.011.

18. McNichol J, Stryhanyuk H, Sylva SP, Thomas F, Musat N, Seewald JS, Sievert SM. 2018. Primary productivity below the seafloor at deep-sea hot springs. Proc Natl Acad Sci U S A 115:6756–6761. https://doi.org/10.1073/pnas.1804351115.

19. Huber JA, Mark Welch DB, Morrison HG, Huse SM, Neal PR, Butterfield DA, Sogin ML. 2007. Microbial population structures in the deep marine biosphere. Science 318:97–100. https://doi.org/10.1126/science.1146689.

20. Meyer JL, Akerman NH, Proskurowski G, Huber JA. 2013. Microbiological characterization of post-eruption "snowblower" vents at Axial Seamount, Juan de Fuca Ridge. Front Microbiol 4:153. https://doi.org/10.3389/fmicb.2013.00153.

21. Akerman NH, Butterfield DA, Huber JA. 2013. Phylogenetic diversity and functional gene patterns of sulfur-oxidizing subseafloor Epsilonproteobacteria in diffuse hydrothermal vent fluids. Front Microbiol 4:185. https://doi.org/10.3389/fmicb.2013.00185.

22. Gulmann LK, Beaulieu SE, Shank TM, Ding K, Seyfried WE, Sievert SM. 2015. Bacterial diversity and successional patterns during biofilm formation on freshly exposed basalt surfaces at diffuse-flow deep-sea vents. Front Microbiol 6:901. https://doi.org/10.3389/fmicb.2015.00901.

23. Han Y, Perner M. 2015. The globally widespread genus Sulfurimonas: versatile energy metabolisms and adaptations to redox clines. Front Microbiol 6:989. https://doi.org/10.3389/fmicb.2015.00989.

24. Stokke R, Dahle H, Roalkvam I, Wissuwa J, Daae FL, Tooming-Klunderud A, Thorseth IH, Pedersen RB, Steen IH. 2015. Functional interactions among filamentous Epsilonproteobacteria and Bacteroidetes in a deep-sea hydrothermal vent biofilm. Environ Microbiol 17:4063–4077. https://doi.org/10.1111/1462-2920.12970.

25. Anderson RE, Reveillaud J, Reddington E, Delmont TO, Eren AM, McDermott JM, Seewald JS, Huber JA. 2017. Genomic variation in microbial populations inhabiting the marine subseafloor at deep-sea hydrothermal vents. Nat Commun 8:1114. https://doi.org/10.1038/s41467-017-01228-6.

26. Mino S, Kudo H, Takayuki A, Sawabe T, Takai K, Nakagawa S. 2014. Sulfurovum aggregans sp. nov., a novel hydrogen-oxidizing, thiosulfate-reducing chemolithoautotroph within the Epsilonproteobacteria isolated from a deep-sea hydrothermal vent chimney at the Central Indian Ridge, and an emended description of the genus Sulfurovum. Int J Syst Evol Microbiol 64:3195–3201. https://doi.org/10.1099/ijs.0.065094-0.

27. Mori K, Yamaguchi K, Hanada S. 2018. Sulfurovum denitrificans sp. nov., an obligately chemolithoautotrophic sulfur-oxidizing epsilon proteobacterium isolated from a hydrothermal field. Int J Syst Evol Microbiol 68: 2183–2187. https://doi.org/10.1099/ijsem.0.002803.

28. Sievert SM, Wieringa EBA, Wirsen CO, Taylor CD. 2007. Growth and mechanism of filamentous-sulfur formation by Candidatus Arcobacter sulfidicus in opposing oxygen–sulfide gradients. Environ Microbiol 9:271–276. https://doi.org/10.1111/j.1462-2920.2006.01156.x.

29. Sievert SM, Hügler M, Taylor CD, Wirsen CO. 2008. Sulfur oxidation at deep-sea hydrothermal vents, p 238–258. In Dahl C, Friedrich CG (ed), Microbial sulfur metabolism. Springer Berlin Heidelberg, Berlin, Germany.

30. Tully BJ, Wheat CG, Glazer BT, Huber JA. 2018. A dynamic microbial community with high functional redundancy inhabits the cold, oxic subseafloor aquifer. ISME J 12:1–16. https://doi.org/10.1038/ismej.2017.187.

31. Galambos D, Anderson RE, Reveillaud J, Huber JA. 2019. Genome-resolved metagenomics and metatranscriptomics reveal niche differentiation in functionally redundant microbial communities at deep-sea hydrothermal vents. Environ Microbiol 21:4395–4410. https://doi.org/10.1111/1462-2920.14806.

32. Fortunato CS, Huber JA. 2016. Coupled RNA-SIP and metatranscriptomics of active chemolithoautotrophic communities at a deep-sea hydrothermal vent. ISME J 10:1925–1938. https://doi.org/10.1038/ismej.2015.258.

33. Dyksma S, Bischof K, Fuchs BM, Hoffmann K, Meier D, Meyerdierks A, Pjevac P, Probandt D, Richter M, Stepanauskas R, Mußmann M. 2016. Ubiquitous Gammaproteobacteria dominate dark carbon fixation in coastal sediments. ISME J 10:1939–1953. https://doi.org/10.1038/ismej.2015.257.

34. Böhnke S, Sass K, Gonnella G, Diehl A, Kleint C, Bach W, Zitoun R, Koschinsky A, Indenbirken D, Sander SG, Kurtz S, Perner M. 2019. parameters governing the community structure and element turnover in Kermadec volcanic ash and hydrothermal fluids as monitored by inorganic electron donor consumption, autotrophic CO2 fixation and 16S tags of the transcriptome in incubation experiments. Front Microbiol 10:2296. https://doi.org/10.3389/fmicb.2019.02296.

35. Wirsen CO, Sievert SM, Cavanaugh CM, Molyneaux SJ, Ahmad A, Taylor LT, DeLong EF, Taylor CD. 2002. Characterization of an autotrophic sulfide-oxidizing marine arcobacter sp. that produces filamentous sulfur. Appl Environ Microbiol 68:316–325. https://doi.org/10.1128/AEM.68.1.316-325.2002.

36. Taylor CD, Wirsen CO. 1997. Microbiology and ecology of filamentous sulfur formation. Science 277:1483–1485. https://doi.org/10.1126/science.277.5331.1483.

37. Roller BRK, Stoddard SF, Schmidt TM. 2016. Exploiting rRNA operon copy number to investigate bacterial reproductive strategies. Nat Microbiol 1: 16160. https://doi.org/10.1038/nmicrobiol.2016.160.

38. Trembath-Reichert E, Butterfield DA, Huber JA. 2019. Active subseafloor microbial communities from Mariana back-arc venting fluids share metabolic strategies across different thermal niches and taxa. ISME J 13: 2264–2279. https://doi.org/10.1038/s41396-019-0431-y.

39. Götz F, Pjevac P, Markert S, McNichol J, Becher D, Schweder T, Mussmann M, Sievert SM. 2019. Transcriptomic and proteomic insight into the mechanism of cyclooctasulfur- versus thiosulfate-oxidation by the chemolithoautotroph Sulfurimonas denitrificans. Environ Microbiol 21:244–258. https://doi.org/10.1111/1462-2920.14452.

40. Seewald JS, Doherty KW, Hammar TR, Liberatore SP. 2002. A new gas-tight isobaric sampler for hydrothermal fluids. Deep Sea Res Pt I 49: 189–196. https://doi.org/10.1016/S0967-0637(01)00046-2.

41. Weiss RF. 1970. The solubility of nitrogen, oxygen and argon in water and seawater. Deep Sea Res and Oceanographic Abstracts 17:721–735. https://doi.org/10.1016/0011-7471(70)90037-9.

42. Pernthaler A, Pernthaler J, Amann R. 2002. Fluorescence In Situ Hybridization and Catalyzed Reporter Deposition for the Identification of Marine Bacteria. Appl Environ Microbiol 68:3094–3101. https://doi.org/10.1128/AEM.68.6.3094-3101.2002.

43. Ishii K, Mussmann M, MacGregor BJ, Amann R. 2004. An improved fluorescence in situ hybridization protocol for the identification of bacteria and

archaea in marine sediments. FEMS Microbiol Ecol 50:203–213. https://doi.org/10.1016/j.femsec.2004.06.015.

44. Sekar R, Fuchs BM, Amann R, Pernthaler J. 2004. Flow sorting of marine Bacterioplankton after Fluorescence in situ hybridization. Appl Environ Microbiol 70:6210–6219. https://doi.org/10.1128/AEM.70.10.6210-6219.2004.

45. Pruesse E, Peplies J, Glöckner FO. 2012. SINA: accurate high-throughput multiple sequence alignment of ribosomal RNA genes. Bioinformatics 28:1823–1829. https://doi.org/10.1093/bioinformatics/bts252.

46. Snaidr J, Amann R, Huber I, Ludwig W, Schleifer KH. 1997. Phylogenetic analysis and in situ identification of bacteria in activated sludge. Appl Environ Microbiol 63:2884–2896. https://doi.org/10.1128/aem.63.7.2884-2896.1997.

47. Quast C, Pruesse E, Yilmaz P, Gerken J, Schweer T, Yarza P, Peplies J, Glöckner FO. 2013. The SILVA ribosomal RNA gene database project: improved data processing and web-based tools. Nucleic Acids Res 41:D590–D596. https://doi.org/10.1093/nar/gks1219.

48. Caporaso JG, Kuczynski J, Stombaugh J, Bittinger K, Bushman FD, Costello EK, Fierer N, Peña AG, Goodrich JK, Gordon JI, Huttley GA, Kelley ST, Knights D, Koenig JE, Ley RE, Lozupone CA, McDonald D, Muegge BD, Pirrung M, Reeder J, Sevinsky JR, Turnbaugh PJ, Walters WA, Widmann J, Yatsunenko T, Zaneveld J, Knight R. 2010. QIIME allows analysis of high-throughput community sequencing data. Nat Methods 7:335–336. https://doi.org/10.1038/nmeth.f.303.

49. Bolyen E, Rideout JR, Dillon MR, Bokulich NA, Abnet CC, Al-Ghalith GA, Alexander H, Alm EJ, Arumugam M, Asnicar F, Bai Y, Bisanz JE, Bittinger K, Brejnrod A, Brislawn CJ, Brown CT, Callahan BJ, Caraballo-Rodríguez AM, Chase J, Cope EK, Da Silva R, Diener C, Dorrestein PC, Douglas GM, Durall DM, Duvallet C, Edwardson CF, Ernst M, Estaki M, Fouquier J, Gauglitz JM, Gibbons SM, Gibson DL, Gonzalez A, Gorlick K, Guo J, Hillmann B, Holmes S, Holste H, Huttenhower C, Huttley GA, Janssen S, Jarmusch AK, Jiang L, Kaehler BD, Kang KB, Keefe CR, Keim P, Kelley ST, Knights D, et al. 2019. Reproducible, interactive, scalable and extensible microbiome data science using QIIME 2. Nat Biotechnol 37:852–857. https://doi.org/10.1038/s41587-019-0209-9.

50. Callahan BJ, McMurdie PJ, Rosen MJ, Han AW, Johnson AJA, Holmes SP. 2016. DADA2: high-resolution sample inference from Illumina amplicon data. Nat Methods 13:581–583. https://doi.org/10.1038/nmeth.3869.

51. Bokulich NA, Kaehler BD, Rideout JR, Dillon M, Bolyen E, Knight R, Huttley GA, Gregory Caporaso J. 2018. Optimizing taxonomic classification of marker-gene amplicon sequences with QIIME 2's q2-feature-classifier plugin. Microbiome 6:90. https://doi.org/10.1186/s40168-018-0470-z.

52. Hammer O, Harper DAT, Ryan PD. 2001. PAST: Paleontological Statistics Software Package for education and data analysis. Palaeontologia Electronica 4:9.